IJABBR- 2014- eISSN: 2322-4827

International Journal of Advanced Biological and Biomedical Research

Journal homepage: www.ijabbr.com

Original Article

Investigating Fluid Mixing in Electro-Osmotic Flow Through Passive Micro-Mixers Having Square and Triangle Barriers

Dina Sezavar[1], Mohadeseh Miri[2*]

[1]*Department of Mechanical Engineering, University of Birjand, Birjand, Iran*
[2]*Department of Mechanical Engineering, University of Zabol, Zabol, Iran*

ARTICLE INFO

Article history:
Received: 05 Sep, 2014
Revised: 25 Oct, 2014
Accepted: 22 Nov, 2014
ePublished: 30 Dec, 2014

Key words:
Electro-osmotic
Passive micro-mixer
Barrier-embedded

ABSTRACT

Objective: In this article, a numerical study is conducted on mixing of two fluids in the liquid phase with two different concentrations of a chemical species in the electro-osmotic flow. **Methods:** The base liquid is an electrolyte which flows in a two-dimensional micro-channel having electrically charged walls. Lorentz electric force, which is used as stimulating flow factor, is created by applying an external electric field on the electric double layer (EDL) aroused by adjacency of electrolyte and charged wall. **Results:** To ensure the convergence of the results obtained from the computer program, equations are solved iteratively until the residual amount after solving each equation is less than machine error and independence of results from the number and location of network nodes is verified for an experimental flow. To increase the mixing efficiency, some square and triangle shaped obstacles are embedded on the micro channel wall. Herein, the fundamental principles for passive mixing as well as the effect of frequency and height of the barriers on mixing efficiency are studied. The obtained results from numerical solving of electro-osmotic flow in micro-channel are compared with the theoretical results and a very good agreement is observed.

1.INTRODUCTION

Scale-down is a novel strategy which recently has attracted great interest in chemical and bioscience analyses. Especially, in the last two decades, scaling down has brought about fabrication of fluid micro-tools. For analyzing the fluid in fluid micro-tools, sometimes it is necessary to mix different volumes of fluid in a small scale. At such small scales, diffusion mechanism is the main mechanism in natural mixing. Due to lack of turbulence within flows passing through fluid micro-tools, mixing of species is more on the basis of molecular diffusion. It is proven that the flux of molecular diffusion in a solution directly depends on the multiplication of the molecular diffusion coefficient (D), Interference level (A), and species concentration gradient (∇C). Aside from the increase in molecular diffusion coefficient (For example, with an increase in temperature) desired enhancement can be performed by maximizing the $A.\nabla C$. In addition to the methods for heightening the diffusion flux, methods that increase the convection flux are also generally employed in mixing tools (Hessel et al, 2004).

The first investigations on passive barrier-embedded micro-mixers was done by Lin et al. who tried to overcome time-consuming mixing of freezing cryogenic liquids and thus the low solidification rate, by putting the cylindrical-shaped obstacles in the path of flow in a micro-channel with a height of 100 μm and width of 10 μm (Lin et al,2003). There are some other experimental studies in this regard. Sheen et al. in 2007 studied triangular barriers and Bhagat et al in 2007 investigated

*Corresponding Author: Mohadeseh Miri, Department of Mechanical Engineering, University of Zabol, Zabol, Iran (mohadeseh_miri@yahoo.com)

the rhombus barriers in a Y-shaped micro-channel (Kumar et al, 2010). In 2008, Chen et al. simulated the mixing characteristics in a two-dimensional electro-osmotic flow and a pressure driven flow through a passive micro-mixer with sine-shaped obstacles, separately (Che and Cha, 2010). In 2008, Wang et al. investigated mixing efficiency in micro-mixers by simulation of two-dimensional electro-osmotic flow using Lattice Boltzmann Method (LBM) (Wang et al, 2008). In 2013, Afonso et al. studied the analytical solution of two-fluid electro-osmotic flows of viscoelastic fluids. They described an analytical model a two-fluid electro-osmotic flow of stratified fluids with Newtonian or viscoelastic rheological behavior (Afonso et al, 2013). Moreover, in 2012, Li et al. showed an analytical solution of transient velocity for electro-osmotic flow of generalized Maxwell fluids through both a micro-parallel channel and a micro-tube, using the method of Laplace transform. Their solution involved analytically solving the linearlized Poisson–Boltzmann equation, together with the Cauchy momentum equation and the general Maxwell constitutive equation (Xiao et al, 2012). Also in 2009 Afonso et al. studied on the Analytical solution of mixed electro-osmotic/pressure driven flows of visco elastic fluids in micro-channels. They shown Analytical solutions are presented for the flow of visco elastic fluids in micron sized ducts, namely between parallel plates and pipes under the combined influence of electro-kinetic and pressure forces using the Debye–Huckel approximation, including the limit case of pure electro-osmotic flow . The studied micro-channel had square obstacles and the effect of height and distance of barriers on mixing efficiency were analyzed. Since the direct channel shows poor performance in mixing in low Reynolds number flows, the present study will discuss mixing characteristics in barrier embedded channels with electro-osmotic flow. Lorentz electric force, which is used as stimulating flow factor, is created by applying an external electric field on the electric double layer (EDL) aroused by adjacency of electrolyte and charged wall. Also numerical simulation will be investigated to analyze the effect of the shape and number of obstacles on the mixing efficiency within the micro-mixer.

2. Physical model and numerical method

The simple rectangular micro-channel has the width of W and the length of L. To simplify the governing equations, the following assumptions have been considered:

(1) An aqueous solution is a Newtonian fluid and non- compressible.
(2) The effects of gravity and buoyancy are ignored.
(3) Two mixing fluid species have the same diffusion coefficients.
(4) There is no chemical reaction.

Steady form of the applied equations to describe the electro-osmotic flow are as follow:

Externally applied electric field distribution within the micro-channel is presented in the form of a two-dimensional Laplace equation.

$$\frac{\partial^2 \phi}{\partial x^2} + \frac{\partial^2 \phi}{\partial y^2} = 0 \qquad (1)$$

Where ϕ is applied as external electric potential.

A Poisson equation governs the electric field distribution within the electric double layer (Region near the walls which contains a non-zero value of the electric potential is called electric double layer, or EDL [9]):

$$\nabla^2 \psi = \frac{2 n_0 z e}{\varepsilon_r \varepsilon_0} \sinh\left(\frac{ze}{k_B T}\psi\right) \qquad (2)$$

Where ψ is the electric potential of EDL, n_0 is the bulk ionic concentration, z is ionic valence number, e is the charge of a proton, ε_r is Dielectric constant of the solution, ε_0 permittivity of vacuum, k_B Boltzmann constant, and T is the absolute temperature.

Modified equations of Navier-Stokes for steady incompressible micro channel are expressed as follows:

$$\nabla . \vec{V} = 0 \qquad (3)$$

$$\rho(\vec{V}.\nabla)\vec{V} = -\nabla P + \mu \nabla^2 \vec{V} + \vec{F}_{EOF} \qquad (4)$$

Where ρ is the fluid density, P is the pressure, and $\vec{V}$ is the velocity vector.

The term $\vec{F}_{EOF}$ implies driving body force in the electro-osmotic flow and is derived from Lorentz equation as follows [9]:

$$\vec{F}_{EOF} = 2 n_0 z e \sinh\left(\frac{ze}{k_B T}\psi\right) \nabla(\psi + \phi) \qquad (5)$$

When two liquids with the same chemical species but different concentrations are being adjacent to be mixed, the concentration distribution of species in the resulting mix in micro-channel can be obtained via the following equation:

$$(\vec{V}.\nabla)C = D\nabla^2 C \qquad (6)$$

The boundary conditions for solving the above equation are illustrated according to figure (1). It should be noted that by placing obstacles in the micro channel wall, boundary conditions will not change.

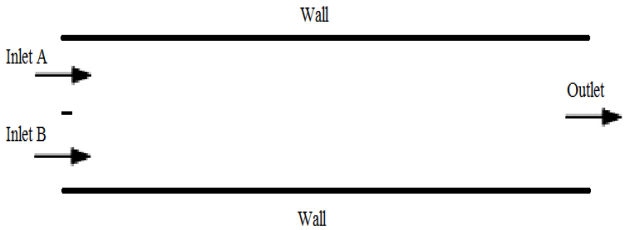

Figure 1: Schematic plan of a simple micro channel

The inlet boundary condition:

$$\frac{\partial \psi}{\partial x}=0, \quad \phi=\phi_{in}, \quad \frac{\partial u}{\partial x}=0, \quad v=0, \quad C=C_{in}, \quad \frac{\partial P}{\partial x}=0 \qquad (7)$$

The outlet boundary condition:

$$\frac{\partial \psi}{\partial x}=0, \quad \phi=\phi_{out}, \quad \frac{\partial u}{\partial x}=0, \quad \frac{\partial v}{\partial x}=0, \quad \frac{\partial C}{\partial x}=0, \quad \frac{\partial P}{\partial x}=0 \qquad (8)$$

Boundary condition on the wall:

$$\psi=\zeta, \quad \frac{\partial \phi}{\partial y}=0, \quad u=0, \quad v=0, \quad \frac{\partial C}{\partial y}=0, \quad \frac{\partial P}{\partial y}=-\rho_e \frac{\partial \psi}{\partial y} \qquad (9)$$

In equations 7 to 9, ϕ_{in} and ϕ_{out} are applied external electric field at the input and outlet of the micro-channel, respectively and ζ is the zeta potential. If two inlet liquids to the micro-mixture are shown by A and B, the corresponding concentrations, are shown by $C_A = 0$ at top inlet and $C_B = 1$ at bottom inlet, respectively. Numerical iterative algorithm functions are as follows: Considering the conservation principle, governing equations are discrete and solved with finite volume method. A staggered grid has been applied in order to avoid any checkered solutions in the velocity and pressure fields. A pressure correction-based iterative algorithm (SIMPLE) is employed for computation.

3. DISCUSSION

Two different geometries in which the mixing of two fluids is investigated are shown in figures (2) and (3). A fluid flow is established from left to right by applying a potential gradient field on positive charged ions inside EDL. It is assumed that there is a uniform negative zeta potential on all parts of the walls. The expansion coefficient of the grid in the vicinity of obstacles is considered $F_x = 1.01$ (along the stream) and $F_y = 1.02$ (perpendicular to the boundary).

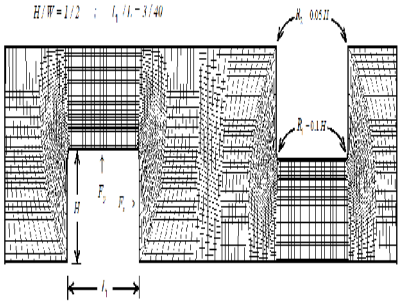

Fig 2. Part of the generated grid on a micro channel with square barriers on the top and bottom of the walls.

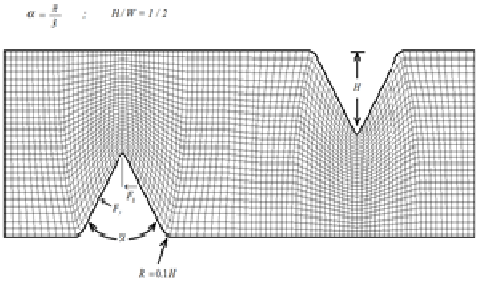

Fig 3. Part of the generated grid on a micro channel with triangle barriers on the top and bottom of the walls.

Table 1.
Physical properties of solution

Parameter	Amount (units)	Parameter	Amount (units)
ζ (zeta potential)	-75 [mv]	(The basis charge of electron) e	$1/6021 \times 10^{-19}$[C]
μ (Dynamic viscosity)	$0/9 \times 10^{-3}$[Pa.s]	k_B (Boltzmann constant)	$1/38 \times 10^{-23}$[J/K]
ρ (Density)	10^{3}[kg/m^3]	C_0 (Molar concentration)	0/001 [mole]
ε_r (Dielectric constant)	78/3	D (Diffusion coefficient of species)	10^{-10} [m^2/ s]
ε_0 (Electric permittivity of vacuum)	$8/854 \times 10^{-12}$ [C/V m]	n_0 (Electrolyte concentration)	$6/02 \times 10^{19}$ [1/ m^3]
z (Number of valence)	1	T (Absolute temperature of the fluid)	298/16 [K]

Other secondary required quantities can be calculated and applied using to the following relationships.

$$n_0 = C_0\ N_A = 0.001 \times 6.02 \times 10^{23} = 6.02 \times 10^{20}\ (1/m^3)$$

$$\Rightarrow \frac{1}{K} = 0.967\ \mu m$$

$$K = 10.41 \times 10^5\ \ 1/m$$

In order to prove the accuracy of the numerical solution, a flow is simulated in a square hole with its movable upper side. The Dirichlet boundary condition is used at all sides of the square. Since this problem is solved for many times, extensive information is reported on the flow field. A good data is reported by Ghia and Shin using FLUENT software data. The fluid flow is simulated with a Reynolds number of 100. The velocity of the moving edge is defined by using *Re* number formulation while the kinematic viscosity is assumed 0.9×10^{-6}. For example, in figure (4) more accurate distribution of the dimensionless velocity along the vertical line is illustrated at *x/L = 0.5*. It is observed that numerical results are in agreement with the solution provided by Ghia and Shin.

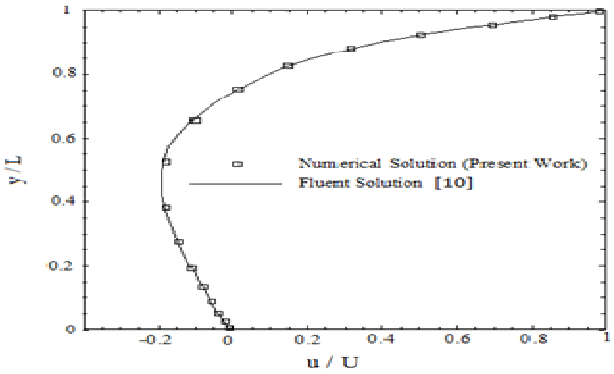

Figure 4. Distribution of dimensionless velocity in *x/L = 0.*

By solving the equation (1) of the external electric field with boundary conditions at the inlet (ϕ_{in} = 62/3) and outlet (ϕ_{out} = 0) of the flow through the micro-mixer, the electric field distribution within the micro channel for four square and triangle shaped barriers will be in the forms of figures (5) and (6).

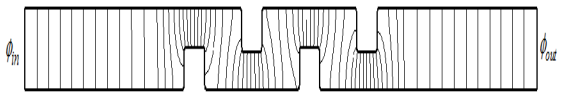

Figure 5. Distribution of external electric field (ϕ) in passive micro mixer with Square obstacles

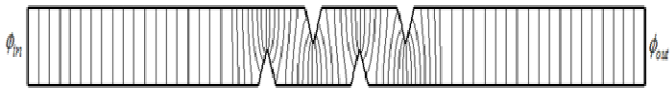

Figure 6. Distribution of external electric field (ϕ) in passive micro mixer with triangle obstacles

It is observed that due to the derivative boundary condition on the walls of the duct, fixed ϕ lines are perfectly perpendicular to the walls of the micro-mixer. Contours of the electric potential field are shown in figures (7) and (8). It can be seen that the electric potential field has a non-zero gradient (Perpendicular to border) only in the electrical double layer (EDL) and outside the EDL, it has a neutral electrical condition. For more clarification, the electrical potential profile and dimensionless velocity profile across the width of micro-channel at x/L =1 are shown in figures (9) and (10), respectively.

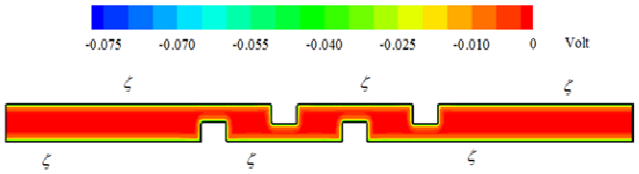

Figure 7. Distribution of electrical potential (ψ) in a passive micro mixer with square obstacles.

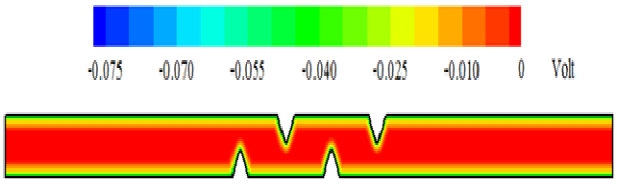

Figure 8. Distribution of electrical potential (ψ) in passive micro mixer with triangle obstacles.

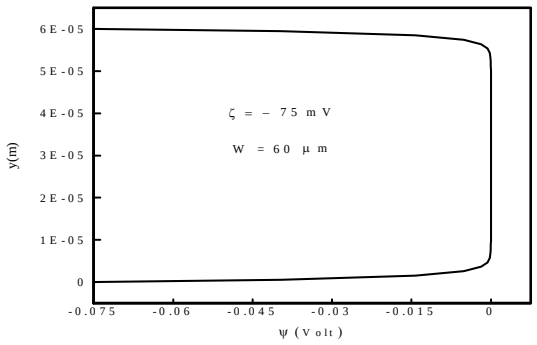

Figure 9. Distribution of electrical potential across the width of micro channel at $\frac{x}{L} = 1$

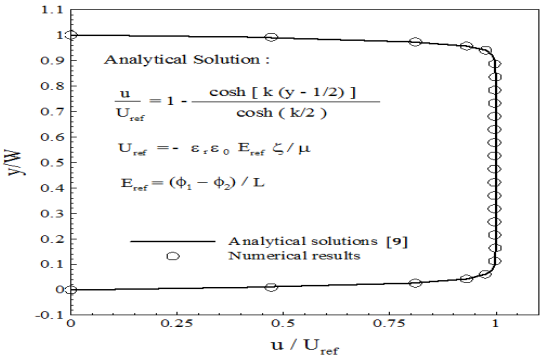

Figure 10. Distribution of dimensionless velocity of an electro-osmotic flow (EOF) between two parallel plates.

It is expected that obstacles on the walls of the micro-channel cause a change in the velocity distribution profile. This transformation can be seen in figure (11) and (12), where the velocity vectors are shown across the micro-channel. When a square obstacle is on the way of the flow, due to the flat area on the top of the obstacle and the presence of two edges, the velocity distribution reveals more changes and the velocity distributions are flat at the inlet and outlet areas, as expected.

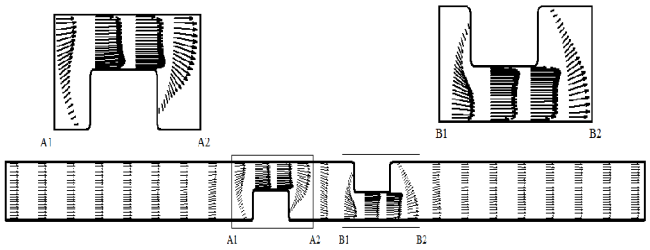

Figure 11. The velocity vectors of the electro-osmotic flow within micro mixer with square obstacles (*Re=0.2*).

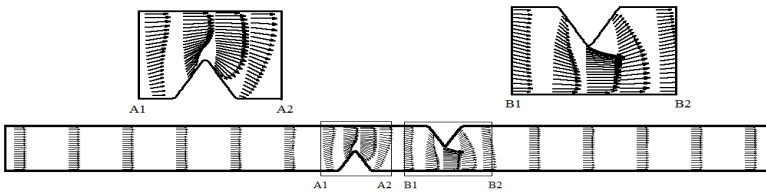

Figure 12. The velocity vectors of the electro-osmotic flow within micro-mixer with triangle obstacles (*Re=0.2*).

Because of the existence of electric force within the electrolyte between positive and negative charges of the walls, a perpendicular pressure gradient is created right next to the walls. Due to the created balance between the pressure gradient and the electric charge along the *y* direction, no motion of the fluid is observed toward the walls. Fig. (13) apparently illustrates the pressure distribution.

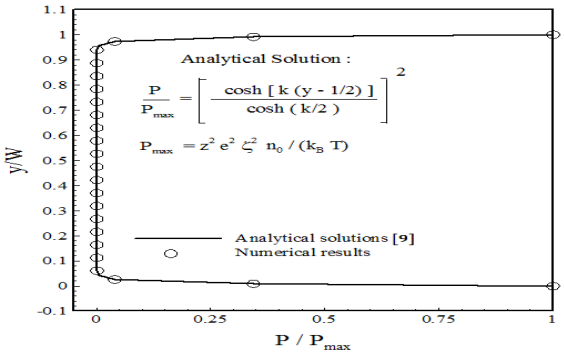

Figure13. Dimensionless pressure distribution across the width of micro-channel at x/L = 1

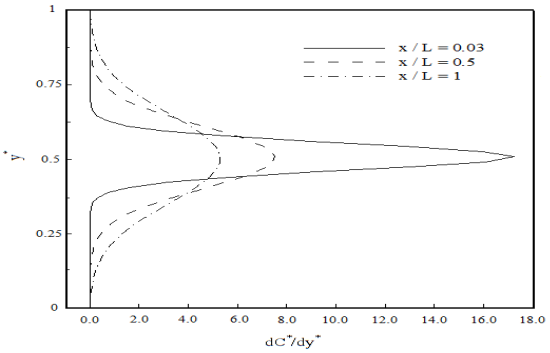

Figure14. Dimensionless concentration gradient of species within the micro-channel

All the parameters except zeta potential (ζ) have constant values. Since the zeta potential across the width of micro-channel have the maximum value, as shown in Fig. (13), P_{max} also occurs on the walls of the micro-mixer

and P / P_{max} at $\frac{y}{W} = 0$ and $\frac{y}{W} = 1$ is equal to 1. Pressure distributions that are plotted at the final section of the both micro-mixers with square and triangle obstacles are the same. The effect of the obstacles on efficiency of mixing of two liquids can be observed in Fig. 14. In Fig. (14), C^* is dimensionless concentration of the mixture that is defined as $C^* = \frac{C}{C_0} - C_\infty$ and also dimensionless width of micro channel is defined as $y^* = \frac{y}{W}$. This figure compares the concentration gradient of species in three different sections from inlet to outlet across the width of micro-channel. It can be observed that the concentration gradient of species across the width of micro-channel has a large value at the entrance section of micro channel ($\frac{x}{L} = 0.03$) and it gets smaller while moving forward to the outlet of micro-channel which represents a more homogeneous concentration of species at the outlet of the micro-channel compared to the inlet.

The mixing efficiency parameter is defined as follow.

$$mixing\ efficiency = \left(1 - \frac{\int_{lower\ surface}^{upper\ surface} \frac{|C^* - C_\infty^*|}{S} ds}{\int_{lower\ surface}^{upper\ surface} \frac{|C_0^* - C_\infty^*|}{W} ds}\right) \times 100\% \quad (10)$$

In this study, the above equation can be simplified as:

$$mixing\ efficiency = \left(1 - 2 \times \int_{lower\ surface}^{upper\ surface} \frac{|C^* - C_\infty^*|}{S} ds\right) \times 100\% \quad (11)$$

Fig. (15) shows the concentration contours of various species in micro-mixers with different numbers of square barriers on the surface. The distance of barriers from each other (d) is 2 times of the width of the micro-mixer ($d = 1/2W$) and also the height of the barrier has been considered as the half the width of the micro-mixer ($h = 0.5W$). Fig. (16) illustrates the distribution of the species concentration across the width of the micro-mixer at the outlet section and compares it in smooth channel (without obstacles) with micro-mixers of different number of square barriers at the wall. It is clear that by increasing the number of obstacles, distribution of species concentration tends to 0.5 which represents a more homogeneous concentration at the outlet of the micro-mixer. For instance, for case of six obstacles, C^* value varies between 0.16 and 0.85, while at the entrance of the channel it has the value of 0 and 1. Fig. (17) displays the mixing efficiency along a smooth micro-mixer (without obstacles) and micro-mixers with different numbers of square barriers at the walls. As can be seen, putting square obstacles at the walls of the micro-channel enhances the mixing efficiency from 24% in a straight channel to 31.6% when one square barrier is embedded on the wall, which obviously reveals the effect of the square barriers in raising the mixing efficiency of the micro-mixer.

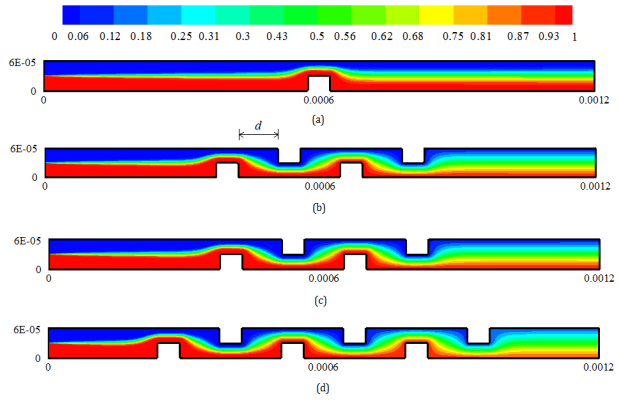

Figure 15. contours of mixed species concentration in micro-mixer in case (a) one, (b) two, (c) four, (d) six square barriers at the wall.

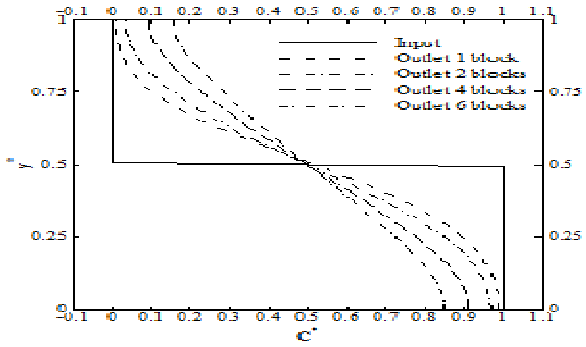

Figure 16. Distribution of species concentration at the inlet and outlet of the micro-mixer of one, two, four and six square barriers at the wall.

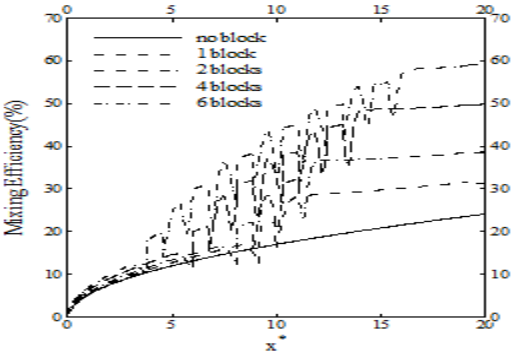

Figure 17. The mixing efficiency of species of the micro-mixer with one, two, four and six square barriers at the wall.

Passive micro-mixers may have different effects on efficiency of fluid mixing, due to their internal shape. In this study the efficiency of mixing in passive micro-mixers with triangular barriers is investigated. Fig. (18) shows the concentration contours in a micro-mixer with different numbers of triangular barriers at the walls. Distance of barriers from each other (d) is 2 times of the width of the micro-mixer ($d = 1/2W$) and also the heights of the barriers are considered half of the width of the micro-mixer ($h = 0.5W$). Fig. 19 displays the mixing efficiency along a smooth micro-mixer (without obstacles) and micro-mixers with different numbers of triangular barriers at the walls. As it can be seen, in the case of six obstacles, the value of c^* varies is between 0.06 and 0.95, while at the entrance of the channel it has the value of 0 and 1.

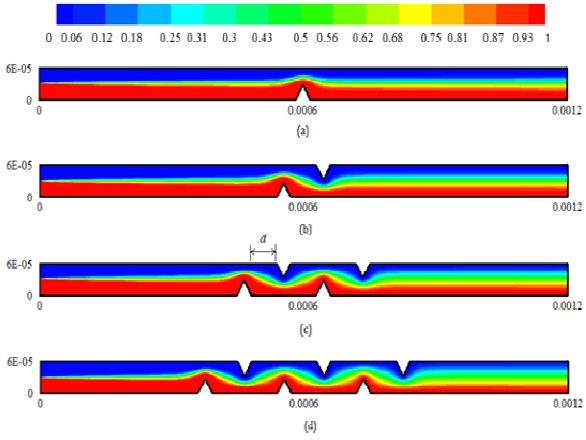

Figure 18. contours of species concentration in the micro-mixer in case of (a) one, (b) two, (c) four, (c) six triangular barriers at the walls.

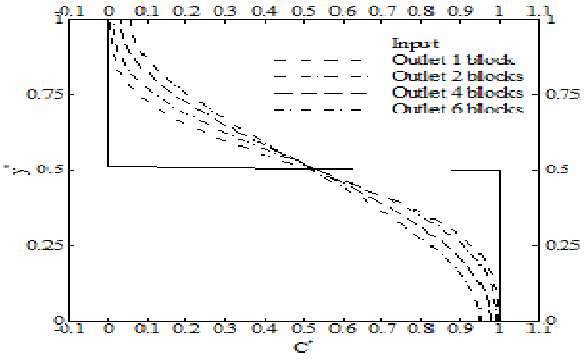

Figure 19: Distribution of species concentration at the inlet and outlet of the micro-mixers with one, two, four and six triangular barriers at the wall.

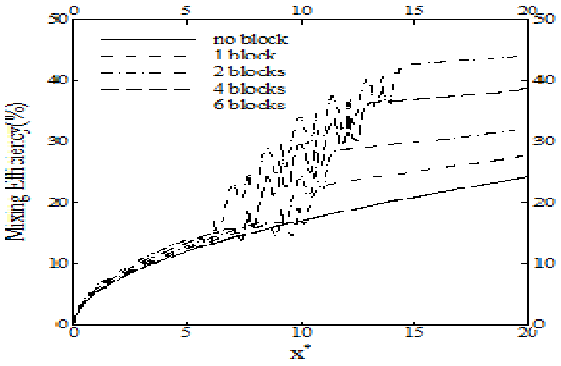

Figure 20: The mixing efficiency of species of the micro-mixer with one, two, four and six triangular barriers at the wall.

Fig.(20) indicates the mixing efficiency along a smooth micro-mixer (without obstacles) and micro-mixers with different numbers of triangular barriers at the walls. As can be seen, putting square obstacles on the walls of the micro-channel enhances the mixing efficiency from 24% in a straight channel to 27.6% when one triangular barrier is embedded at the wall. As it can be observed, the mixing efficiency can reach the value of 44% by embedding six triangular barriers at the wall. The passive micro-mixer can be changed in the structure by using different heights of barriers. Fig. (21) shows the concentration contours in the micro-mixer with square barriers with heights of $h^* = 0.333$, $h^* = 0.5$, $h^* = 0.667$ and $h^* = 0.833$ in the case of four barriers on the walls. The dimensionless height of barriers is defined as $h^* = h / W$. By increasing the height of the barrier which narrows the passing section of the fluid, ∇C rises sharply and therefore the mixing efficiency improves. Fig. (22) shows the distribution of mixing species concentration at the outlet section of a straight channel (without obstacles) and also indicates the effect of different heights of square barriers. Fig. (23) illustrates the mixing efficiency along straight mixing and also the effect of different heights of square barriers. As it can be clearly observed, mixing efficiency increases by embedding four square obstacles of $h^* = 0.333$ within the micro-mixer from 24% in the straight channel to 43.9%. Enhancement in efficiency will continue to 77/3% by raising the height of the square barriers to $h^* = 0.833$.

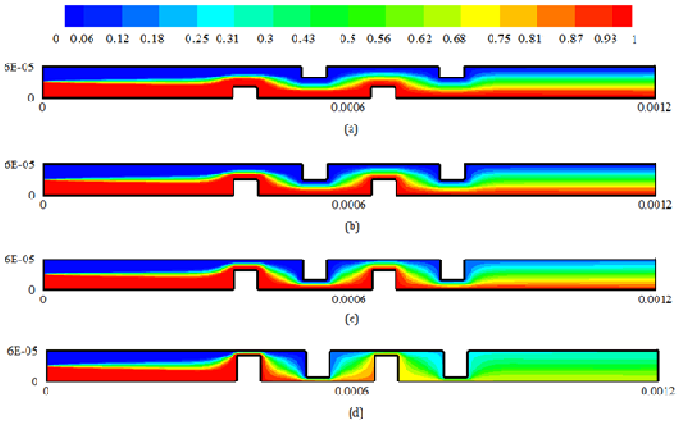

Figure21. contours of species concentration in a micro-mixer with square barriers of different heights

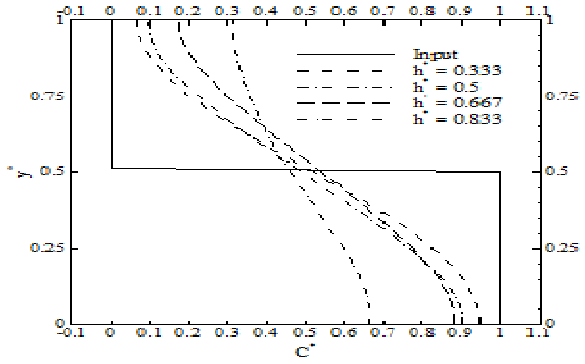

Figure 22. Distributions of species concentration at the inlet and outlet sections of a micro-mixer with square barrier of different heights

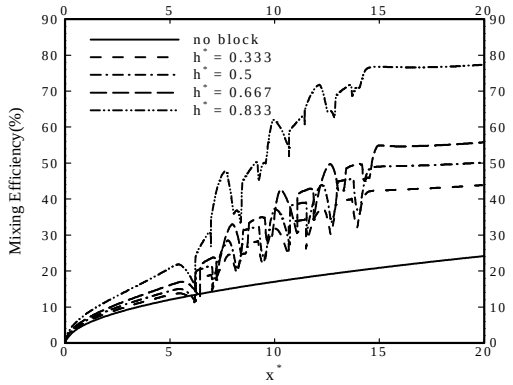

Figure 23. The mixing efficiency of the micro-mixer with square barriers of different height

Fig. (22) indicates concentration contours in a micro-mixer with triangular barriers in presence of four barriers in the flow direction with heights of $h^* = 0.333$, $h^* = 0.5$, $h^* = 0.667$ and $h^* = 0.833$. In the micro-mixer with triangular barriers, two mixing liquids are less exposed to the extreme ∇C compared to square ones since triangular barriers have less upper surface compared to square barriers. Therefore, it is expected that triangular barriers reveal less mixing efficiency. Fig. (25) indicates the distribution of mixing species concentration at the outlet section of a straight channel (without obstacles) and also indicates the effect of different heights of triangular barriers. Fig. (26) shows the mixing efficiency along straight mixing and also the effect of different heights of triangular barriers. As it can be seen, the mixing efficiency is increased by embedding four triangular obstacles of $h^* = 0.333$ within the micro-mixer from 24% in the straight channel to 37.4%. This improvement in efficiency will continue to 62% by raising the height of triangular barriers to $h^* = 0.833$.

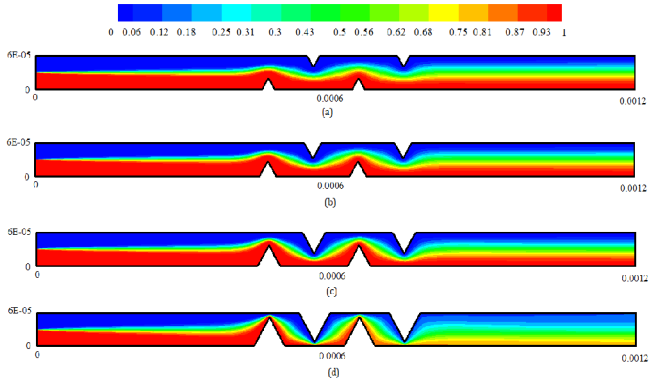

Figure 24. contours of species concentration in a micro-mixer with triangular barriers of different heights.

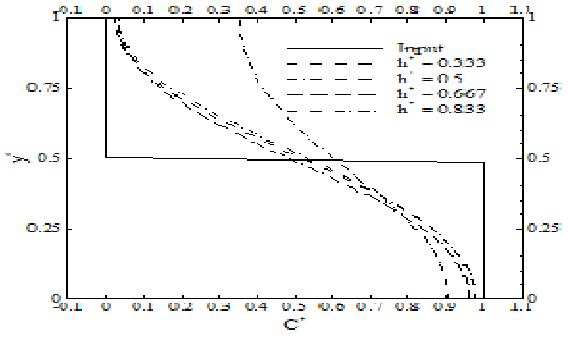

Figure 25. Distributions of species concentration at the inlet and outlet sections of a micro-mixer with triangular barrier of different heights

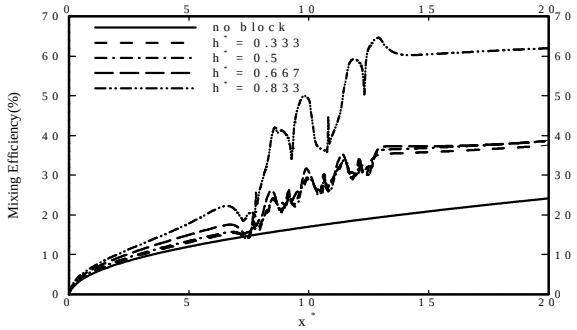

Figure 26. The mixing efficiency of the micro-mixer with triangular barriers of different height

Examining figures (23) and (26) reveals the greater effect of square barriers on the mixing efficiency of the two liquids compared to the triangular barriers.

CONCLUSION

In this paper, the mixing phenomenon of two fluids passing through a micro-channel is investigated. In order to improve the mixing efficiency of the two input fluids to the micro-channel, two different patterns of square and triangular shaped barriers were embedded on the internal surface of the micro-channel. Moreover, the effects of changes in height and number of obstacles on the mixing efficiency were examined. The results indicate higher mixing efficiency with square obstacles on the internal surface of micro-mixer compared to triangular ones. Furthermore, it can be observed that for both types of barriers, the heights of barriers cause more enhancement in the mixing efficiency rather than their number. Although the effects of obstacles on improvement of mixing efficiency in passive micro-mixers were investigated, it should always be considered that the minimum flow rate within the micro-channel is not less than required flow rate for the particular application of the micro-channel.

REFERENCES

Hessel,V., Löwe, H., Schönfeld, F., "Micromixers a review on passive and active mixing principles", Chemical Engineering Science, vol 60 , pp 2479 – 2501, 2004.

Lin, Y., Gerfen, G. J., Rousseau, D. L., Yeh, S. R., "Ultrafast microfluidic mixer and freeze–quenching device", Analytical Chemistry ,75, pp 5381–5386, 2003.

Kumar, V., Paraschivoiu, M., Nigam, K. D. P., "Single-phase fluid flow and mixing in microchannels", Journal of Chemical Engineering Science ,Article in Press, 2010.

Che, C. K., Chao, C., "Electrokinetically-driven flow mixing in microchannels with wavy surface", Journal of Colloid and Interface Science 312, pp 470–80, 2007.

Wang, D., Summers, J. L., Gaskell, P. H., "Modelling of electrokinetically driven mixing flow in microchannels with patterned blocks", Computers and Mathematics with Applications ,55 , pp 1601–1610, 2008.

A.M. Afonso, M.A. Alves, F.T. Pinho, " Analytical solution of two-fluid electro-osmotic flows of viscoelastic fluids", Journal of Colloid and Interface Science 395, pp. 277–286, 2013

Xiao-Xia Li, Ze Yin, Yong-Jun Jian, Long Chang, Jie Su, Quan-Sheng Liu, " Transient electro-osmotic flow of generalized Maxwell fluids through a microchannel" , Journal of Non-Newtonian Fluid Mechanics 187–188, pp. 43-47, 2012.

A.M. Afonso, M.A. Alves, F.T. Pinho, " Analytical solution of mixed electro-osmotic/pressure driven flows of viscoelastic fluids in microchannels" , Journal of Non-Newtonian Fluid Mechanics 159, pp. 50-63, 2009.

Mirbozorgi, S. A., Niazmand, H., Renksizbulut, M., "Electro-Osmotic Flow in Reservoir Connected Flat Microchannels With Non-Uniform Zeta Potential", Journal of Fluids Engineering 128 , pp 1133–43, 2006.

Ghia, U., Ghia, K. N., Shin, C. T., "High-*Re* solutions for incompressible flow using the Navier–Stokes equations and a multigrid method", Journal of Computational Physics; 48, pp 387–411, 1982.